Cell Host & Microbe
Article

An Identical miRNA of the Human JC and BK Polyoma Viruses Targets the Stress-Induced Ligand ULBP3 to Escape Immune Elimination

Yoav Bauman,[1] Daphna Nachmani,[1] Alon Vitenshtein,[1] Pinchas Tsukerman,[1] Nir Drayman,[2] Noam Stern-Ginossar,[1] Dikla Lankry,[1] Raizy Gruda,[1] and Ofer Mandelboim[1,*]
[1]The Lautenberg Center for General and Tumor Immunology, The BioMedical Research Institute Israel Canada of the Faculty of Medicine
[2]Department of Hematology
Hebrew University-Hadassah Medical School, Jerusalem 91120, Israel
*Correspondence: oferm@ekmd.huji.ac.il
DOI 10.1016/j.chom.2011.01.008

SUMMARY

The human polyoma viruses JCV and BKV establish asymptomatic persistent infection in 65%–90% of humans but can cause severe illness under immunosuppressive conditions. The mechanisms by which these viruses evade immune recognition are unknown. Here we show that a viral miRNA identical in sequence between JCV and BKV targets the stress-induced ligand ULBP3, which is a protein recognized by the killer receptor NKG2D. Consequently, viral miRNA-mediated ULBP3 downregulation results in reduced NKG2D-mediated killing of virus-infected cells by natural killer (NK) cells. Importantly, when the activity of the viral miRNA was inhibited during infection, NK cells killed the infected cells more efficiently. Because NKG2D is also expressed by various T cell subsets, we propose that JCV and BKV use an identical miRNA that targets ULBP3 to escape detection by both the innate and adaptive immune systems, explaining how these viruses remain latent without being eliminated by the immune system.

INTRODUCTION

Polyoma viruses are small DNA viruses that are highly prevalent in the human population. Among this family of viruses, the human polyoma viruses BKV and JCV establish a subclinical persistent infection in 65%–90% of all humans (Eash et al., 2006). Infection by these two viruses is asymptomatic under normal conditions; however, under immunosuppressive conditions, the persistent virus infection can cause severe illnesses (Jiang et al., 2009). JCV is known as the causative agent of progressive multifocal leukoencephalopathy (PML), a rapidly progressive disease of the central nervous system (CNS), which is fatal in about 90% of all patients (Jiang et al., 2009; Eash et al., 2006). The virally induced pathogenesis of BKV is polyomavirus-induced nephropathy (PVN), which causes severe renal allograft dysfunction and ultimate graft loss (Nickeleit et al., 1999). Thus, it is conceivable to assume that under normal conditions JCV and BKV developed mechanisms, which so far remain unknown, to enable their coexistence with their human hosts. The diseases induced by both BKV and JCV have no efficient treatment, and therefore the understanding of how these viruses escape detection by the immune system is essential, as it may lead to the development of therapeutic approaches for the treatment of the above mentioned viral diseases.

Polyoma viruses contain a small genome and are thought to encode around six proteins only (Johnson, 2010; Eash et al., 2006). Importantly, both JCV and BKV encode two miRNAs that were so far demonstrated to target the viral protein T antigen (Tag) (Sullivan et al., 2005; Seo et al., 2008). MiRNAs are noncoding small RNA molecules that are found in almost all organisms and are involved in nearly every biological process (Bartel, 2009). MiRNAs mainly bind to the 3′ untranslated regions (3′UTRs) of protein-coding mRNA transcripts, and such binding leads to inhibition of protein translation, which is often followed by mRNA degradation (Bartel, 2009; Guo et al., 2010). In general, the activity of miRNAs is moderate, and they operate as fine-tuners of biological processes (Baek et al., 2008). Nevertheless, the activity of a particular miRNA can have a dramatic effect on the function of a certain protein. Furthermore, because each miRNA can target around 300 genes, the manipulation of miRNAs activity may also lead to dramatic and global changes in the function of many proteins (Baek et al., 2008).

MiRNAs are also involved in immune regulation (O'Connell et al., 2010). We have previously shown that three different viral miRNAs, encoded by three different herpesviruses (EBV, KSHV, and HCMV), can selectively target the stress-induced ligand MICB and not other stress-induced ligands such as ULBPs or MICA (Stern-Ginossar et al., 2007; Nachmani et al., 2009). MICB is recognized by the powerful killer receptor NKG2D, which is expressed by NK cells and by other immune cells (Raulet, 2003). Thus, the downregulation of MICB by the viral miRNAs results in the escape of the infected cells from the NKG2D-mediated immune recognition and elimination (Nachmani et al., 2009; Stern-Ginossar et al., 2007). Since both human polyomaviruses and herpesviruses coexist with the human host (Speck and Ganem, 2010; Boothpur and Brennan, 2010; Eash et al., 2006), because they can cause severe illnesses under immunosuppressive conditions and because BKV and JCV encode miRNAs, we hypothesized that the BKV and the JCV

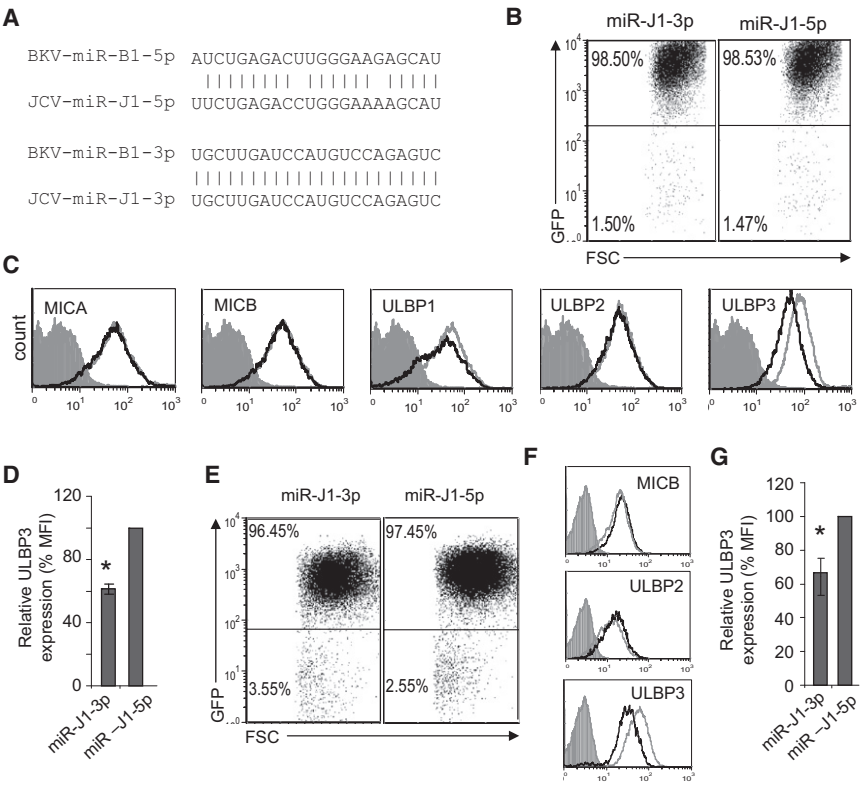

Figure 1. Specific Downregulation of ULBP3 in Cells Overexpressing the BKV and JCV miRNAs

(A) Schematic representation of the 3p* and the 5p arms-derived miRNAs of JCV and BKV. (B and E) Percentages (indicated in the figure) of GFP-positive BJAB cells (B) and RKO (E) cells transduced with the indicated miRNAs. MiR-J1-3p is the BKV-miR-B1-3p/JCV-miR-J1-3p, and the control miR-J1-5p is the miRNA derived from the parallel 5p arm of the pre-miRNA of JCV. (C and F) FACS analysis for the expression of all detectable NKG2D ligands by BJAB cells (C) and by RKO cells (F), following transduction either with the BKV-miR-B1-3p/JCV-miR-J1-3p (miR-J1-3p, black open histogram) or the control miR-J1-5p (gray open histogram). The filled gray histogram represents the staining of the second mAb only. Figure shows one representative experiment out of three performed. (D and G) Quantification of the ULBP3 downregulation, in BJAB (D) and in RKO (G) cells. The percentages of ULBP3 downregulation (% MFI), in cells transduced with miR-J1-3p, were calculated relative to cells transduced with the control miR. Shown are mean values ± SD. Statistically significant differences are indicated (*$p < 0.005$, by one-tailed t test). Error bars (SD) are derived from the result of three independent experiments.

miRNAs may also target the NKG2D ligands to escape the NKG2D-mediated elimination.

Here we describe an immune evasion mechanism of the human polyoma viruses and demonstrate that through the specific downregulation of ULBP3, a ligand for NKG2D, BKV, and JCV escape immune cell attack. These findings may explain how these viruses remain latent in most of the human population without being eliminated by the immune system.

RESULTS

The 3p* miRNAs of BKV and of JCV Specifically Downregulate ULBP3 Expression

Whether human polyoma viruses developed mechanisms to escape immune recognition is still unknown. Since we have demonstrated that three different herpes viruses, HCMV, EBV, and KSHV, all escape NKG2D-mediated recognition through the usage of distinctive miRNAs that target MICB (Nachmani et al., 2009; Stern-Ginossar et al., 2007), we speculated that the miRNAs of BKV and JCV might also target the stress ligands of NKG2D. To test this hypothesis and to avoid the usage of computer algorithms which are currently still inaccurate, we undertook a practical unbiased approach in which we transduced BJAB cells that endogenously express numerous NKG2D ligands with lentiviral vectors expressing the miRNAs of JCV and BKV. We used lentiviral vectors expressing the less abundant miRNA (3p* [Seo et al., 2008]) derived from the 3p arm of the pre-miRNAs of JCV and of BKV (BKV-miR-B1-3p/JCV-miR-J1-3p), which is identical between these two viruses (we therefore designated it miR-J1-3p, Figure 1A and throughout the manuscript). In addition we also generated two additional lentiviral vectors containing the 5p-derived miRNAs of BKV and JCV, which are different between the viruses (Figure 1A). All of the lentiviral vectors also contain a GFP cassette that enables us to monitor for the transduction efficiency, which was in general very high (Figure 1B and all other transductions throughout the manuscript). As can be seen in Figures 1C and 1D, a substantial decrease (around 40%, Figure 1D) in the expression of ULBP3 was observed in BJAB cells overexpressing miR-J1-3p, while the other miRNAs, derived from the 5p arm of JCV, or BKV, (miR-J1-5p and miR-B1-5p respectively), had no effect (Figures 1C and 1D and data not shown). Furthermore, other control viral miRNAs such as ebv-BART1 or kshv-miR-K12-3 had no effect on the ULBP3 downregulation (data not shown). Therefore, to use a biologically relevant control, miR-J1-5p was used as a negative control miRNA in all of the following figures. The reduction in ULBP3 expression was specific, as no change in the levels of all other NKG2D ligands, MICA, MICB, ULBP1, and ULBP2, which are present on cell surface of BJAB cells, was observed (Figure 1C). To further corroborate these observations, we transduced another cell line, RKO, which endogenously expresses ULBP3, ULBP2, and MICB with the same lentiviral vectors mentioned above. An effective transduction was observed (Figure 1E), and around 30% reduction in the endogenous ULBP3 expression was noticed in the presence of miR-J1-3p, also in this cell line (Figures 1F and 1G).

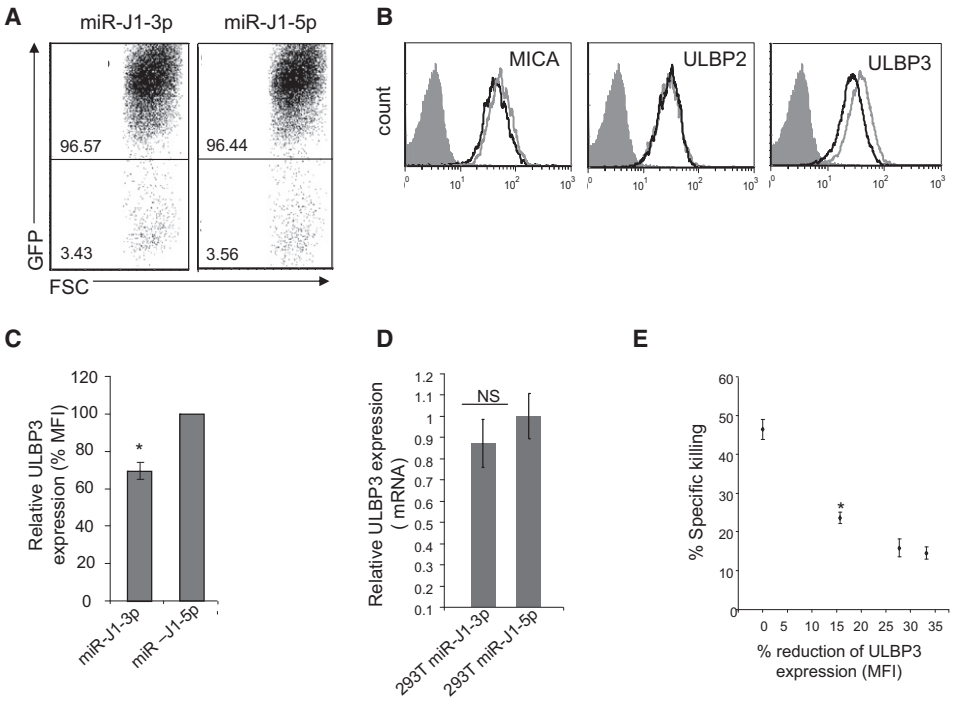

Figure 2. Investigating the Mechanisms of miR-J1-3p-Mediated Reduction of ULBP3 Expression

(A) Percentages (indicated in the figure) of GFP-positive 293T cells transduced with the indicated miRNAs.

(B) FACS analysis of all detectable NKG2D ligands' expression by 293T cells, following transduction with miR-J1-3p (black open histogram), or with the control miR (gray open histogram). The filled gray histogram represents the staining of the second mAb only. Figure shows one representative experiment out of three performed.

(C) Quantification of ULBP3 expression in 293T cells transduced with miR-J1-3p relative to 293T cells transduced with the control miR. Statistically significant differences are indicated (*$p < 0.005$, by one-tailed t test). Error bars (SD) are derived from the result of three independent experiments.

(D) QPCR analysis of the mRNA levels of ULBP3 found in 293T cells transduced with miR-J1-3p, or with miR-J1-5p as indicated. Specific ULBP3 Taq-man primers were used. Error bars (SD) are derived from triplicates. Results are representative of three independent experiments.

(E) Subtle changes in ULBP3 expression leads to a significant reduction in NK-mediated killing. 293T cells were transduced with various shRNAs directed against ULBP3 (three in total), or with a control shRNA (used as reference shRNA, indicated in the figure as 0% reduction). The reduction in the MFI of ULBP3 expression was calculated relative to the MFI levels of ULBP3 expression in cells tranduced with the control scramble sequence. The various 293T cells, expressing the various shRNAs, were then labeled and incubated for 5 hr with bulk NK cells at an effector:target (E:T) ratio of 6:1. Shown are mean values ± SD. Statistically significant differences are indicated (*$p < 0.005$, by one-tailed t test). Error bars (SD) are derived from triplicates.

Investigating the Mechanisms of miR-J1-3p-Mediated ULBP3 Downregulation

We have previously demonstrated that the cellular and the viral miRNAs that were found to modulate MICB expression are probably operating through inhibition of translation (Stern-Ginossar et al., 2007, 2008; Nachmani et al., 2009; Nachmani et al., 2010). To investigate the mechanisms by which miR-J1-3p mediates the reduction of ULBP3 expression and to reinforce our above observations, we transduced another cell line, 293T, with the viral miRNAs mentioned above (Figure 2A). The 293T cell line endogenously expresses ULBP3, MICA, and ULBP2 (Figure 2B). As can be seen in Figure 2B, and in agreement with the above results (Figure 1), around 30% reduction in ULBP3 expression was observed also in 293T cells expressing miR-J1-3p, relative to the control miR, miR-J1-5p (Figures 2B and 2C). Because the downregulation of ULBP3 expression was not associated with a decrease in the mRNA levels of ULBP3, as detected by quantitative real-time PCR (QPCR) analysis (Figure 2D), we concluded that miR-J1-3p probably reduces ULBP3 levels through inhibition of translation.

The miRNA-mediated reduction of ULBP3 (Figures 1 and 2) and of MICB (Nachmani et al., 2009, 2010; Stern-Ginossar et al., 2007, 2008) is moderate. Nevertheless, we demonstrated before (Nachmani et al., 2009, 2010; Stern-Ginossar et al., 2007, 2008) that such moderate reduction in the stress-induced ligand MICB is functional. To quantify the extent of the ULBP3 downregulation that is needed to obtain a significant reduction in NK cytotoxicity, we transduced 293T cells with various shRNAs directed against ULBP3 (three in total, Figure 2E), or with a control shRNA construct which includes a scramble sequence. We obtained several 293T clones expressing various levels of ULBP3 (the expression levels of all other NKG2D ligands remained unchanged [data not shown]), and we calculated the percentages of ULBP3 reduction relative to the expression of the ULBP3 on 293T cells transduced with the scrambled shRNA (designated as 0% reduction in Figure 2E). Interestingly, we observed that even subtle changes in ULBP3 expression (as low as 15% reduction, Figure 2E) were sufficient to cause a substantial reduction in NK cytotoxicity.

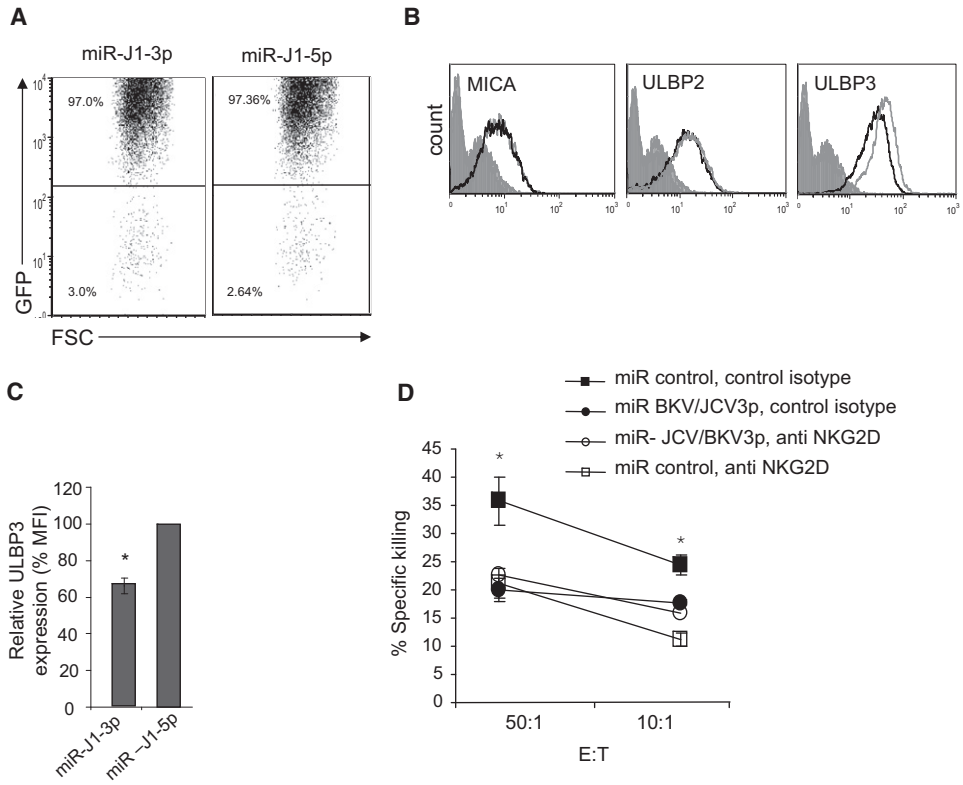

Figure 3. The miRNA-Mediated ULBP3 Downregulation Resulted in Reduced NKG2D-Mediated Killing

(A) Percentages (indicated in the figure) of GFP-positive U87 cells transduced with miR-J1-3p and miR-J1-5p.

(B) FACS analysis of all detectable NKG2D ligands expressed by U87 cells, transduced with lentiviral vectors encoding either miR-J1-3p (black open histogram), or the control miRNA miR-J1-5p (gray open histogram). The filled gray histogram represents the staining of the second mAb only.

(C) Quantification of ULBP3 expression in U87 cells, transduced with miR-J1-3p relative to U87 cells transduced with the control miR. Shown are mean values ± SD. Statistically significant differences are indicated (*$p < 0.005$, by one-tailed t test). Error bars (SD) are derived from the result of three independent experiments.

(D) Reduced NKG2D-mediated killing of U87 cells overexpressing miR-J1-3p. Bulk NK cells were preincubated either with anti-NKG2D mAb (empty circle or square) or with isotype-match control mAb (filled circle or square). Labeled U87 cells expressing either miR-J1-3p (circle) or miR-J1-5p (square) were then added and incubated for 5 hr at the indicated effector:target (E:T) ratios. Shown are mean values ± SD. Statistically significant differences are indicated (*$p < 0.005$, by one-tailed t test). Error bars (SD) are derived from triplicates. Figure shows one representative experiment out of three performed.

The Viral miRNA-Mediated Reduction of ULBP3 Expression Leads to Reduced NKG2D-Dependent Killing

We next aimed to study the functional outcome of the reduced ULBP3 expression mediated by miR-J1-3p. For that purpose we transduced another cell line, the U87 cell line (a glioblastoma cell line, representing the cells that are naturally infected by the JC virus), with the lentiviral vectors encoding the different miRNAs mentioned above (Figure 3A). In agreement with the above results, around 30% reduction in the expression of ULBP3, but not of ULBP2 or MICA, was observed when miR-J1-3p was overexpressed in these cells, whereas the control miR had no effect (Figures 3B and 3C).

Next, we performed NK cytotoxicity assays against the transduced U87 cells. As can be seen in Figure 3D, and in agreement with the reduction of ULBP3 expression mediated by miR-J1-3p, a significant decrease in the U87 killing was observed when miR-J1-3p, but not the control miR, was present in the cells. The miRNA-mediated reduction of NK cytotoxicity resulted from reduced NKG2D recognition, as killing of all cells was equivalent when the NKG2D interactions were blocked (Figure 3D).

MiR-J1-3p Directly Binds to the 3′UTR of ULBP3

Our next aim was to determine whether the miR-J1-3p-mediated ULBP3 downregulation is direct and whether it is executed through its binding to 3′UTR of ULBP3. Since the 3′UTR sequence of the ULBP3 mRNA was unknown, we cloned ULBP3 (NM_024518.1) together with its unknown UTR from a cDNA library made of U87 cells and determined its sequence (Figure 4A). We next used the online RNAhybrid program (http://bibiserv.techfak.unibielefeld.de/rnahybrid/submission.html) to scan for potential binding sites of miR-J1-3p and identified such a site, which contains a full seed match for miR-J1-3p, located between nucleotides 267 and 290 (Figure 4B). In contrast, and in agreement with the above observations, no seed-containing sites were identified for the miRNAs derived from the 5p arms of both JCV and BKV. To test whether miR-J1-3p indeed targets this specific site, we preformed dual luciferase reporter assays. We generated two firefly luciferase constructs, one containing the wild-type 3′UTR of ULBP3, and a second one containing the 3′UTR in which we mutated the seed region of the predicted miR-J1-3p binding site (Figure 4C).These constructs were transiently transfected into cells

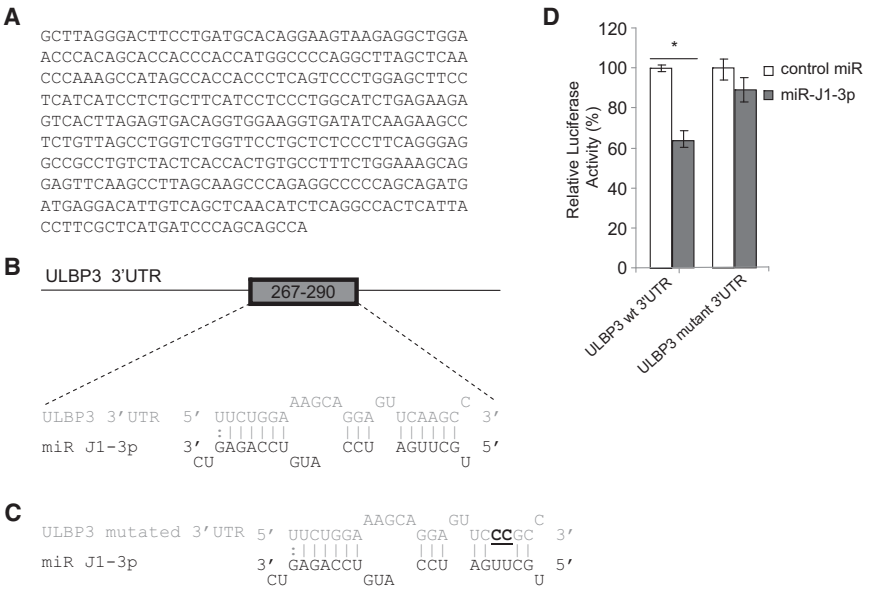

Figure 4. The JCV and BKV miRNAs Directly Bind to the 3′UTR of ULBP3

(A) The sequence of the 3′UTR of the ULBP3 gene obtained from a cDNA library made from the U87 cell line.

(B) A schematic representation of the 3′UTR of ULBP3 and the predicted binding site for BKV-miR-B1-3p/JCV-miR-J1-3p miRNAs.

(C) Alignment of miR-J1-3p and the mutated 3′UTR of ULBP3 (double point mutations in the predicted seed region are marked in bold and are underlined).

(D) The figure demonstrates relative luciferase activity after transfection of the indicated reporter plasmids: wild-type (WT), or mutant ULBP3 3′UTR, into MDA-MB-231 cells expressing either miR-J1-3p (gray) or the control miR-J1-5p (white). Firefly luciferase activity was normalized to Renilla luciferase activity and then normalized to the average activity of the control reporter. Shown are mean values ± SD. Statistically significant differences are indicated (*$p < 0.001$) by one-tailed t test). Error bars (SD) are derived from triplicates. Figure shows one representative experiment out of three performed.

that had been transduced with miR-J1-3p, or with a control miRNA. As can be seen in Figure 4D, a decrease in luciferase activity was observed only in cells expressing miR-J1-3p, while the mutations in the 3′UTR of ULBP3 abolished this observed effect. Thus, both JCV and BKV express an identical miRNA that specifically targets the 3′UTR of ULBP3, reduces its expression, and consequently diminishes the NKG2D-mediated killing.

MiR-J1-3p Reduces ULBP3 Expression during Infection to Escape NKG2D Recognition

Our next aim was to demonstrate that the miRNA-mediated reduction of ULBP3 expression plays a significant role during viral infection. For an unknown reason, despite numerous attempts, the use of various virus stocks (purchased from ATCC) and various cell lines, we were unable to infect cells with BKV. However, because JCV and BKV express the same relevant miRNA, we continued our analysis with the JCV only. All cell lines (RKO and BJAB, Figure 1; 293T, Figure 2; and U87, Figure 3) that we used here to demonstrate the miR-J1-3p effect express ULBP3 on the cell surface prior to the miRNA transduction. Although the expression of ULBP family members could be detected under normal conditions on healthy cells (Eagle et al., 2009), it might be possible that the cells which are naturally infected in vivo with JCV do not express ULBP3 before the infection. To investigate whether JCV infection will affect ULBP3 expression, we infected U87 cells with 512 hemagglutination units (HAUs) of JCV and verified that the cells were indeed infected by western blot analysis to detect the presence of the JCV large T antigen in the infected cells (Figure 5A). Next we performed QPCR analysis to determine the mRNA levels of the NKG2D ligands (ULBP3, ULBP2, and MICA), expressed by U87 cells, before and after JCV infection. As can be seen in Figure 5B, significant increase in the mRNA levels of ULBP3 and MICA, but not of ULBP2, was observed in the infected cells compared to uninfected cells.

We next aimed to determine whether this elevation in mRNA levels of MICA and ULBP3 will result in increased protein expression and whether miR-J1-3p could prevent this elevation. Again, U87 cells were infected with 512 HAU of JCV, and since the JCV miRNAs (both the 3p* and the 5p) were shown to be expressed around 72 hr postinfection (Seo et al., 2008), we started monitoring ULBP3 expression at that time. No significant change in the levels of MICA, ULBP2, or ULBP3 expression was observed at this time point, 72 hr postinfection (data not shown), despite the induction of mRNA for MICA and ULBP3 (Figure 5B). In contrast, 6 days following the infection we noticed a reduction in ULBP3 expression in the infected cells (Figure 5C), which correlated with the increased expression of miR-J1-3p (around 50-fold above control, Figure 5D). The expression of ULBP2 or MICA remained unchanged (Figure 5C), indicating that the observed effect is specific. The expression of ULBP3 remained low in the following days until U87 cells lost viability. To further examine the mechanism leading to ULBP3 downregulation following JCV infection, we performed western blot analysis to detect the ULBP3 protein levels before and after the infection. As could be seen in Figure 5E and despite the elevation in the ULBP3 mRNA levels following infection (Figure 5B), around 70% reduction in the ULBP3 protein level was observed following the infection. Finally, we have also determined that the reduction in ULBP3 expression during infection resulted in a parallel reduction in NK cytotoxicity (Figure 5F).

Inhibition of miR-J1-3p Activity during Infection Restored ULBP3 Expression and Enhanced NK Killing of the JCV-Infected Cells

Our final aim was to block the miR-J1-3p function and to demonstrate directly that this miRNA indeed facilitates the downregulation of ULBP3 during infection. We therefore generated an antiviral miRNA sponge directed against miR-J1-3p. Sponges directed against a particular miRNA contain multiple adjacent binding sites for the miRNA of interest and thus function as

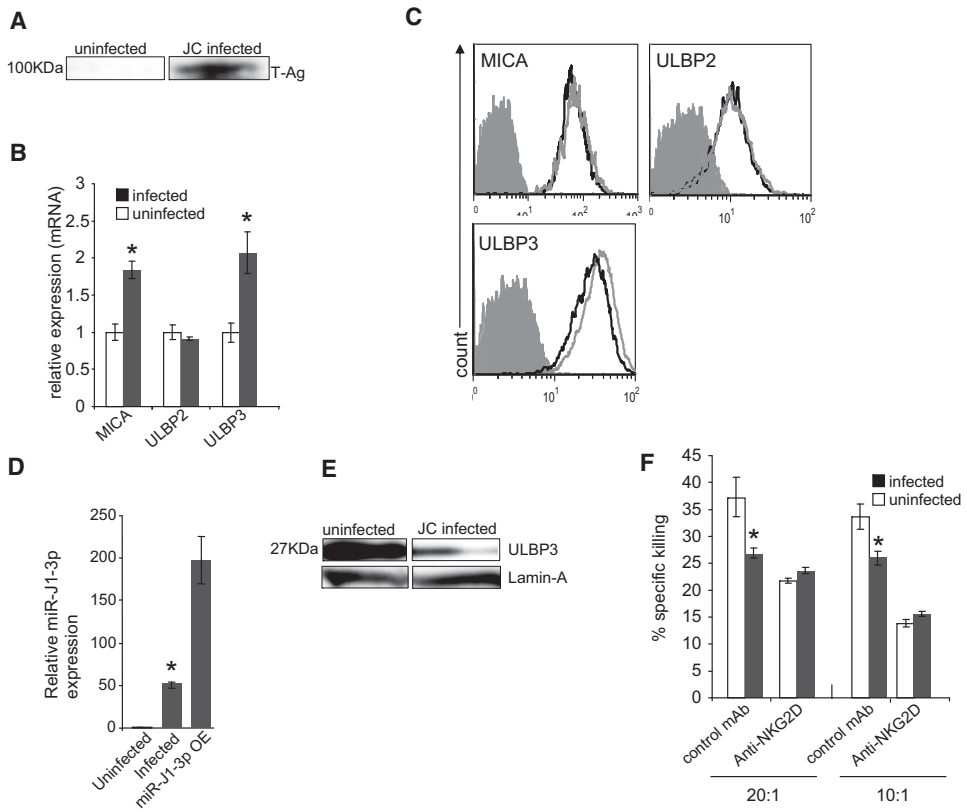

Figure 5. The JCV miRNA miR-J1-3p Reduced ULBP3 Expression during JCV Infection

(A) Western blot analysis of T-antigen (T-ag) protein expression in uninfected cells (left lane), or in JCV-infected U87 cells (right lane). Results are representative of two independent experiments.

(B) QPCR analysis of the mRNA level of ULBP3, ULBP2, and MICA following JCV infection of U87 cells. Specific Taq-man primers were used. Statistically significant differences are indicated (*$p < 0.02$ by one-tailed t test). Error bars (SD) are derived from triplicates. Results are representative of three independent experiments.

(C) FACS analysis of ULBP3, ULBP2, and MICA expression in U87 cells infected with JCV (black open histogram) and on uninfected cells (gray open histogram), 6 days following infection. The filled gray histogram represents the staining of the second mAb only.

(D) QPCR analysis of viral miR-J1-3p miRNA expression, 6 days following JCV infection of U87 cells. U87 cells transduced with lentiviral vector encoding miR-J1-3p were used as positive control. Statistically significant differences are indicated (*$p < 0.02$ by one-tailed t test). Error bars (SD) are derived from triplicates. Results are representative of three independent experiments.

(E) Western blot analysis of ULBP3 protein levels in uninfected U87 cells (left lane), or in JCV-infected cells (right lane). Lower bands in each lane represent the Lamin A protein control. These Lamin controls also serve as controls for (A). Results are representative of two independent experiments.

(F) U87 cells infected with JC virus exhibit reduced NKG2D-mediated NK killing. Bulk NK cells were preincubated either with anti-NKG2D mAb or with isotype control. Infected (gray bars) or uninfected (white bars) U87 cells were then added and incubated for 5 hr at the indicated effector:target (E:T) ratios. Shown are mean values ± SD. Statistically significant differences are indicated (*$p < 0.03$, by one-tailed t test). Error bars (SD) are derived from triplicates. Figure shows one representative experiment out of three performed.

"decoy transcripts" that sequester the miRNA from targeting its original target (Ebert et al., 2007). The antiviral miRNA sponge was cloned in the 3′UTR of GFP reporter cassette, and the sponge was transduced into U87 cells. This strategy enabled us not only to monitor for the transduction efficiency, but also to detect the sponge activity during infection, as the sponge absorption of the relevant miRNA will lead to a reduction in the GFP intensity. Uninfected or JCV-infected U87 cells were transduced with the sponge directed against miR-J1-3p or with a control sponge (the transduction of the sponge directed against miR-J1-3p into U87 cells did not alter ULBP3 expression, or affected the NK-mediated cytotoxicity of uninfected cells [see Figure S1 available online]). The GFP and ULBP3 expression levels were determined as infection progressed. As shown in Figures 6A and 6B, the infected cells transduced with the sponge directed against miR-J1-3p indeed showed a very prominent decrease in the GFP intensity as compared either to U87 cells transduced with a control sponge or to uninfected cells expressing miR-J1-3p sponge. This indicated that the JCV miRNA was absorbed during infection. Importantly, the sequestration of the JCV miRNA by the anti-miR-J1-3p sponge resulted in increased expression of ULBP3, whereas no change was observed either in ULBP2 or in MICA expression (Figure 6C).

In general, and as also observed throughout the paper, the miRNA effect is moderate (Baek et al., 2008). We also demonstrated here that the moderate ULBP3 downregulation mediated by miR-J1-3p was noticed on the entire cell population (see Figures 1–3 and 5) and that even 15% reduction in ULBP3

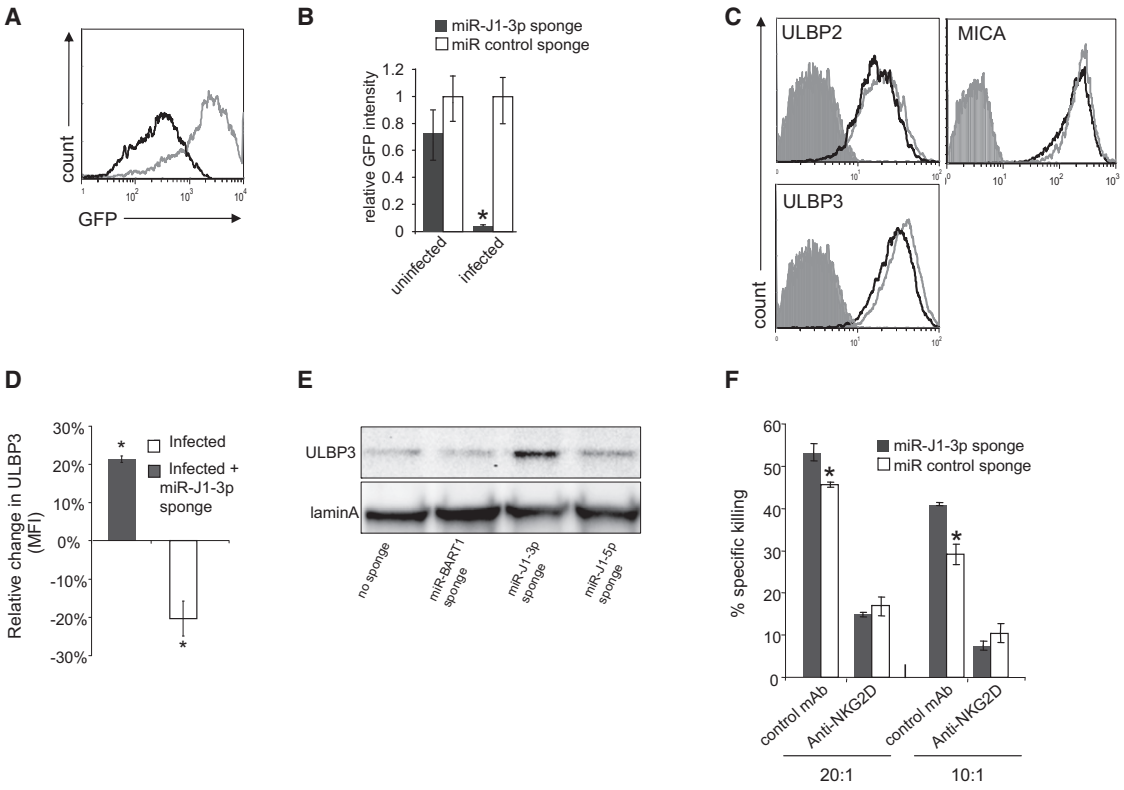

Figure 6. Inhibition of miR-J1-3p Activity during Infection Restored ULBP3 Expression and Enhanced NK Killing of the JCV-Infected Cells

(A) FACS analysis of the GFP intensity in U87 cells transduced either with lentiviral vector encoding for sponge directed against miR-J1-3p (black open histogram), or with a control sponge (EBV-miR-BART1-5p, gray open histogram).

(B) Relative GFP intensity of JCV-infected and uninfected cells transduced with sponge for miR-J1-3p (gray column), or with the miR BART1-5p sponge (white column). Shown are mean values ± SD. Statistically significant differences are indicated (*$p < 0.008$, by one-tailed t test). Error bars (SD) are derived from the result of three independent experiments.

(C) FACS analysis of ULBP3, ULBP2, and MICA expression by infected U87 cells transduced by lentiviral vector encoding sponge against miR-J1-3p (gray open histogram),or control sponge (EBV-miR-BART1-5p, black open histogram). The filled gray histogram represents the staining of the second mAb only.

(D) Quantification of ULBP3 downregulation (infected and transduced with sponge against miR-J1-3p compared to control sponge) and upregulation (infected compared to uninfected). Statistically significant differences are indicated (*$p < 0.03$, by one-tailed t test). Error bars (SD) are derived from three independent experiments.

(E) Western blot analysis for the expression of ULBP3 in infected cells transduced with the indicated anti-miRNA sponge (x axis), 6 days following infection. The Lamin A protein was used as loading control. Results are representative of two independent experiments.

(F) Bulk NK cells were preincubated either with anti-NKG2D mAb or with isotype control mAb. Infected U87 cells transduced with sponge against JCV-miR-J1-3p (gray bar) or with control sponge (white bar) were then added and incubated for 5 hr at the indicated effector:target (E:T) ratios. Shown are mean values ± SD. Statistically significant differences are indicated (*$p < 0.02$, by one-tailed t test). Error bars (SD) are derived from triplicates. Figure show one representative experiment out of three performed. (See also Figure S1.)

expression can lead to a significant reduction in NK cytotoxicity (Figure 2). Nevertheless, to make sure that the moderate effect observed during infection is indeed significant, we repeated the infections and the sponge experiments several times. Figure 6D summarizes the results of the downregulation of ULBP3 expression mediated by miR-J1-3p and the sponge-mediated upregulation of ULBP3, observed during infection. Interestingly, around 20% reduction of ULBP3 expression (as measured by MFI intensity) was observed during infection, and this downregulation was almost completely reversed by the anti-miR-J1-3p sponge activity (Figure 6D), indicating that the observed moderate effect is reproducible and significant. Because we observed a 70% downregulation of ULBP3 expression in western blot analysis, following infection (Figure 5E) and to strengthen our observations we have also assayed the miR-J1-3p sponge effect on ULPB3 expression by using western blot analysis. For that purpose and to make this experiment more biologically relevant, we generated another sponge which is directed against miR-J1-5p. U87 cells were infected as indicated above, and 72 hr postinfection the cells were transduced with a control irrelevant miR-BART1 sponge, with sponge directed against miR-J1-5p and with the miR-J1-3p sponge, or with no sponge. Importantly, around 40% elevation in the ULBP3 expression was observed only with the miR-J1-3p sponge (Figure 6E), indicating that indeed miR-J1-3p functions during JCV infection to reduce ULBP3 expression. Finally, we demonstrated that the anti-miR-J1-3p sponge-mediated upregulation of ULBP3 had functional implications, as it resulted in increased NKG2D-mediated recognition and killing of the infected cells (Figure 6F).

All together, we show that by using identical miRNAs, JCV and BKV downregulte the stress-induced ligand ULBP3 to escape the NKG2D-mediated elimination.

DISCUSSION

In this report we describe an immune evasion mechanism of human polyoma viruses. We also uncover a cellular gene which is targeted by the miRNAs of human polyoma viruses and demonstrate that a viral miRNA is able to target a stress-induced ligand of the ULBP family.

We have undertaken an unbiased practical approach and not a computational based strategy to determine whether indeed the JCV and BKV miRNAs target the stress-induced ligands of NKG2D. This approach was proven to be successful, not only because the computer algorithms that are presently available to predict miRNA targets are highly inaccurate, but also because the 3′UTR of ULBP3 was unknown and thus would have been missed by using a computational approach.

The miRNAs of JC, BK, and of simian virus 40 (SV40) are derived from homologous pre-miRNA hairpins, in which both arms are processed into mature miRNAs that downregulate the viral Tag (Seo et al., 2008; Sullivan et al., 2005). Although the miRNA derived from the 3p arm is considered as the star miRNA, in the sense that it is less abundant than the miRNA derived from the 5p arm, this star miRNA was functional in downregulating the viral Tag (Seo et al., 2008). In agreement with this observation, we demonstrate here that miR-J1-3p (the star miRNA of BKV and JCV) is functional also in downregulating a host gene, ULBP3. Moreover, we found that miR-J1-3p, despite being a star miRNA, is expressed in quite significant levels above background, and that such expression levels were sufficient for the ULBP3 downregulation.

Because all polyoma viruses miRNAs, so far discovered, are located antisense to the viral Tag, researchers speculated that the only function of these miRNAs might be to target this protein (Cullen, 2009; Seo et al., 2008; Umbach and Cullen, 2009). However, as both cellular and viral miRNAs are estimated to target around 300 genes (Skalsky and Cullen, 2010), this assumption seemed to us unlikely. Our hypothesis was that polyoma viruses miRNAs might target additional genes that would be essential for the life cycle of these viruses. This hypothesis was further supported by the observations that the miRNAs of some herpes viruses are also found antisense to a particular viral gene; however, they could still downregulate the expression of other genes (Boss et al., 2009). One notable example with this regard is the HCMV miR-UL112, which is located antisense to the viral UL114 gene and downregulates not only this protein (Stern-Ginossar et al., 2009) but also MICB (Stern-Ginossar et al., 2007) and the viral gene IE72 (Grey et al., 2007). A fascinating question to which the answer is currently unknown is how these miRNAs that are placed antisense to the viral genes acquire the ability to also target cellular genes.

Interestingly, the targeting of the Tag by the SV40 miRNAs was shown to affect CTL responses against peptides derived from the Tag (Sullivan et al., 2005). Whether the Tag downregulation by the miRNAs of JCV and BKV would also affect CTL activity is still unknown. However, it is logical to assume that targeting of the Tag by BKV and JCV miRNA will result in escape from CTL attack. Thus, by using miRNAs, JCV and BKV would escape the detection of both the innate and adaptive immune systems. Furthermore, since NKG2D is expressed by many immune cells including innate NK cells and various T cells subsets, we suggest that by using a single miRNA, the human polyoma viruses may escape the NKG2D-mediated detection and elimination of both the innate and adaptive immune systems.

As mentioned above, MICB is the only known NKG2D ligand targeted by the miRNAs derived from the herpes viruses HCMV, KSHV, and EBV (Nachmani et al., 2009; Stern-Ginossar et al., 2007). In contrast, as we show here, the miRNAs of BKV and JCV target ULBP3 only. Thus, we wondered why the miRNAs of polyoma and herpes viruses target different stress-induced ligands. An analogous question might be why the NKG2D receptor has so many different ligands (eight in total [Champsaur and Lanier, 2010]). We think that the answer to both questions is that these different stress-induced ligands and the opposing viral mechanisms were coevolved due to a host-pathogen "arm race." Thus, the upregulation of the different stress ligands might be related either to the different cell types which are infected by polyoma and herpes viruses, or alternatively, to the life cycle of the different viruses. The viruses, on the other hand, developed specific miRNA-based mechanisms to interfere with the expression of the specific stress ligands induced by each of the viruses.

The stress-induced ligands of human and mouse are different, and ULBP3 (or other human stress-induced ligands) does not exist in the mouse. Thus, the miRNAs-based mechanisms used by both polyoma and herpes viruses to escape immune detection are one of the nicest examples for how human viruses that coevolved with humans for millions of years target stress ligands which are unique to humans. Because the stress ligands are different in human and mice, it is almost impossible to find a satisfactory in vivo model to study whether the miRNA-mediated reduction of ULBP3 would be indeed significant in vivo during the course of authentic infection. We think, however, that our results strongly suggest that, indeed, this is the case.

The miRNAs effect is, in general, moderate (Baek et al., 2008), and the ULBP3 reduction during infection was moderate as well. Importantly, however, such moderate downregulation resulted in decreased killing of the infected cells. Furthermore, the reduction in the ULBP3 protein levels following infection is actually greater than the ULBP3 reduction observed on the cell surface. An intrinsic property of ULBP3 and of other NKG2D ligands such as MICB or MICA is their swift induction upon stress (Champsaur and Lanier, 2010), and indeed we demonstrate that the mRNA levels of ULBP3 and MICA are induced during JCV infection and that, in contrast, the ULBP3 protein levels are reduced. Thus, the miR-J1-3p viral miRNA not only reduces the expression of ULBP3 which is already present on the cell surface but also prevents the translation of the newly synthesized ULBP3 mRNA, following infection. Indeed, western blot analysis for the expression of ULBP3 protein following infection reveled around 70% reduction in ULBP3 expression, whereas the miRNA-mediated surface downregulation of ULBP3 following infection was limited to around 20% only. Furthermore, the anti-miR-J1-3p sponge activity resulted in around 20% elevation of ULBP3 expression on the cell surface and 40% elevation of ULBP3 protein expression.

Despite the elevation in the mRNA levels of MICA and ULPB3 following infection, no elevations in the levels of MICA and ULBP3 were observed on the surface of infected cells at any time point following the infection. On the contrary, we demonstrate here that the miRNA of JCV downregulates ULBP3 expression, at 6 days postinfection. These results suggests that other possible mechanisms of posttranscriptional control including inhibition of translation, rapid degradation of newly translated proteins, or sequestration inside the cell might also operate in the infected cells, to prevent the expression of the stress-induced ligands, similar to protein-based mechanisms used by HCMV and KSHV (Dunn et al., 2003).

It was shown recently that human polyoma viruses proteins, RNA, and DNA are found in many human tumors (Moens and Johannessen, 2008), suggesting that these viruses might contribute to tumorigenesis processes. Although this area of research is still highly speculative, our finding may suggest that viral components might be essential not only for tumor transformation, but also for tumor escape from the NKG2D-mediated elimination. The understanding that ULBP3 plays a dominant role during JCV and BKV infection may lead to the development of antiviral drugs aiming either at antagonizing the miRNA effects or upregulating the expression of ULBP3 in polyoma virus-infected cells and tumors.

EXPERIMENTAL PROCEDURES

Lentiviral Constructs, Production, and Transduction

RNA artificial hairpins that function as orthologs of pre-miRNA hairpins were generated by using the pTER vector (van de Wetering et al., 2003). Two complementary specific oligonucleotides (Table S1) were annealed, phosphorylated using T4 polynucleotide kinase, and inserted into the pTER vector as was previously described (van de Wetering et al., 2003). The artificial hairpin and H1 RNA polymerase III promoter were then excised from the vector and cloned into the lentiviral vector SIN18-pRLL-hEFlap-E-GFP-WRPE. The vector also contains GFP cassette, thus allowing the simultaneous expression of both the reporter GFP and the relevant miRNA. Sponge constructs were generated by annealing the oligonucleotides, phosphorylating them using T4 polynucleotide kinase, and inserting them into the pcDNA3 vector (Invitrogen). The sponges were excised and cloned into the lentiviral vector SIN18-pRLL-hE-Flap EGFP-WRPE (Xu et al., 2001), downstream to the GFP cassette. Each sponge consists of six adjacent binding sites for the relevant viral miRNA, separated by a 4 nt spacer. The sequences of the sponge's binding site are as follows: sponge anti-miR-J1-3p (5′ to 3′), GACTCTGGACTACATCAAGCA; sponge anti-miR-bart1-5p (control), CACAGCACGTCAGAACACTAAGA. Lentiviral vectors were produced by transient three-plasmid transfection protocol. The pMDG envelope expression cassette (3.5 μg), the gag-pol packaging construct (6.5 μg), and the relevant vector construct (10 μg) were transfected into 293T cells using the LT1 transfection reagent (Mirus Bio LLC, Madison, WI). Two days after transfection, the supernatants containing viruses were collected and filtered. These viruses where then used to transduce cells in the presence of polybrene (5 μg/ml). ShRNAs for ULBP3 were obtained from Sigma-Aldrich in the pLKO.1 plasmid. Lentiviral vectors were produced by using the three-plasmid transient transfection method as described above. Transduced 293T cells were grown in medium supplemented with 1ug/ml puromycin. The ShRNA sequences directed against ULBP3 were as follows: clone #1, GCCAGGTGGATCAGAAGAATT; clone #2, CTTCTTCAAGATGG TCTCAAT; clone #3, CGCTCACTCTCTCTGGTATAA.

Cytotoxicity Assays and NK Cell Preparation

The cytotoxic activity of NK cells against various targets was assessed in 5 hr 35S release assays as described (Mandelboim et al., 1996). The final concentration of the blocking antibodies was 2.5 mg/ml. NK cells were isolated from peripheral blood using the Human NK Cell Isolation Kit and the autoMACS instrument (Miltenyi Biotec) according to the manufacturer's instructions. The NK purity was 100% as determined by FACS analysis. The spontaneous release in all assays was always less than 15% of the total release and is subtracted from the calculation of the percentages of lysis. Percentages of killing were calculated as follows: (CPM sample − CPM spontaneous)/(CPM total − CPM spontaneous)*100.

Cells, Viruses, and Antibodies

The BJAB, U87, 293T, RKO, and MDA–MB-321 cell lines were used. Anti-MICA, anti-MICB, anti-ULBP1-3, and anti-NKG2D antibodies were all purchased from R&D Systems (Minneapolis). ULBP3 antibody for western blotting was purchased from R&D (catalog MAB15171). The anti-SV40 Tag antibody (pab416) that cross-reacts with JCV Tag was purchased from Abcam (catalog ab16879) and was used for western blotting. The anti-CD99 (12E7) was used as an isotype control. Anti-CD56 antibody (Becton Dickinson) and anti-CD3 (biolegend) were used to determine NK purity. JC (MAD-4, catalog VR-1583) and BK virus (Cat.VR-837) were purchased from the ATCC. JC virus was propagated in COS-7 for 7 days, at 37°C. Cells were grown in minimum Eagle's medium supplemented with 2% fetal bovine serum. Seven days later, the infected cells together with supernatant were freeze-thawed six times, and virus titers were determined by hemagglutination assay as described (Liu and Atwood, 2001). Briefly, human red blood cells of type O donors were added to 2-fold dilution series of virus (preincubated with 0.25% of sodium deoxycholate) in a U-shaped microtiter plate. Virus titer was determined according to the highest dilution in which hemagglutination was still visible. The human glioblastoma cell line U87 was infected with 512 HAUs of JC virus for 1 hr at 37°C in reduced (2%) sera.

Real-Time PCR of miR-J1-3p

Total RNA was isolated by using the Tri-Reagent (Sigma) and treated with RNase-free DNase-Turbo (Ambion). The treated total RNA (1 μg) was polyadenylated by poly(A) polymerase (PAP) at 37°C for 1 hr in a 20 μl reaction mixture using the Poly(A) Tailing Kit (Ambion). After phenol-chloroform extraction and ethanol precipitation, the RNA was dissolved in diethylpyrocarbonate (DEPC)-treated water. It then was reverse transcribed with mMLV Reverse Transcriptase (Invitrogen) and with 0.5 μg of poly(T) adaptor (3′ rapid amplification of complementary DNA ends [RACE] adaptor using the FirstChoice RLM-RACE kit; Ambion) according to the manufacturer's instructions. Quantitative PCR was used to measure miRNA expression was as follows: 2 μl of cDNA was mixed with 200 μM of both the forward and reverse primers in a final volume of 10 μl and mixed with 10 μl of 2× DyNAmo SYBR Green qPCR (Finnzymes). 5S rRNA and U6 snRNA were used as the endogenous reference genes for PCR quantification. The reverse primer was a 3′ adaptor primer (3′RACE outer primer in the First Choice RLM-RACE kit), and the forward primer was designed based on the entire miRNA sequence. For miR-J1-3p, 5′-TGCTTGAT CCATGTCCAGAGTC-3′. QPCR for the expression of ULBP3, MICA, and ULBP2 mRNA was conducted with specific commercial Taq man primers (Applied Biosystems).

DNA Constructs and Luciferase Assay

For the firefly luciferase vector, we used the pGL3 control vector (Promega). The 3′UTR of ULBP3 was amplified by PCR from U87 cell line cDNA library and inserted into XbaI site immediately downstream to a stop codon. The inserts and their proper orientation were confirmed by sequencing. The primers used to amplify ULBP3 3′UTR were as follows: forward, 5′-TCTCTAG AGGCTTAGGGACTTCCTGA-3′; reverse, 5-TGGCTGCTGGGATCATGATCTA GAGA-3′. For the generation of the mutated ULBP3-3′UTR plasmid, we included a double point mutation in the seed region of binding site using an additional set of primers: forward, 5-AAGCAGGAGTTCCCGCCTTAGCA AG-3′; and reverse, 5′-CTTGCTAAGGCGGGAACTCCTGCTT-3′.

MDA-MB-321 cells were plated in 24-well plates were transfected with 100 ng of a Firefly luciferase reporter vector and 5 ng of the control Renilla luciferase pRL-CMV (Promega) using the LT1 transfection reagent (Mirus), at a final volume of 0.5 ml. Firefly and Renilla luciferase activities were measured consecutively with the Dual-Luciferase Assay System (Promega) 48 hr following transfection. Firefly luciferase activity was normalized to Renilla luciferase activity and then normalized to the average activity of the control reporter.

Western Blot Analysis

Cells were counted and lysed in buffer containing 0.6% SDS and 10 mM Tris (pH 7.4). Proteins concentration in each sample was determined by Bradford method. Equal volumes of samples containing equal protein concentrations were then run on 12.5% Tris-HCl gels, then transferred onto nitrocellulose and incubated for 1 hour with 5% milk. Membranes were incubated overnight with primary Ab; for the blotting of ULBP3, anti-ULBP3 mAb in 3%BSA (1:500) was used. For the blotting of JC T-antigen, anti-Tag mAb in 3% BSA (1:50) was used. Anti-mouse-HRP (Jackson Laboratory) was used as secondary antibody.

SUPPLEMENTAL INFORMATION

Supplemental Information includes one figure and one table and can be found with this article at doi:10.1016/j.chom.2011.01.008.

ACKNOWLEDGMENTS

This study was supported by grants from the Israeli Science Foundation, The Israeli Science Foundation (Morasha), The Croatia Israel Research Grant, The MOST-DKFZ Research grant, and The European Consortium (MRTN-CT-2005); and by the Rosetrees trust, the Israel Cancer Association (20100003), the ICRF professorship grant, and the Association for International Cancer Research (AICR) (all to O.M.). O.M. is a Crown professor of Molecular Immunology. Y.B. performed all experiments, analyzed the data, and wrote the paper. D.N., A.V., P.T., N.D., N.S.-G., D.L., and R.G. all contributed critical help and reagents. O.M. supervised the project.

Received: August 5, 2010
Revised: October 28, 2010
Accepted: January 14, 2011
Published: February 16, 2011

REFERENCES

Baek, D., Villen, J., Shin, C., Camargo, F.D., Gygi, S.P., and Bartel, D.P. (2008). The impact of microRNAs on protein output. Nature *455*, 64–71.

Bartel, D.P. (2009). MicroRNAs: target recognition and regulatory functions. Cell *136*, 215–233.

Boothpur, R., and Brennan, D.C. (2010). Human polyoma viruses and disease with emphasis on clinical BK and JC. J. Clin. Virol. *47*, 306–312.

Boss, I.W., Plaisance, K.B., and Renne, R. (2009). Role of virus-encoded microRNAs in herpesvirus biology. Trends Microbiol. *17*, 544–553.

Champsaur, M., and Lanier, L.L. (2010). Effect of NKG2D ligand expression on host immune responses. Immunol. Rev. *235*, 267–285.

Cullen, B.R. (2009). Viral and cellular messenger RNA targets of viral microRNAs. Nature *457*, 421–425.

Dunn, C., Chalupny, N.J., Sutherland, C.L., Dosch, S., Sivakumar, P.V., Johnson, D.C., and Cosman, D. (2003). Human cytomegalovirus glycoprotein UL16 causes intracellular sequestration of NKG2D ligands, protecting against natural killer cell cytotoxicity. J. Exp. Med. *197*, 1427–1439.

Eagle, R.A., Jafferji, I., and Barrow, A.D. (2009). Beyond stressed self: evidence for NKG2D ligand expression on healthy cells. Curr. Immunol. Rev. *5*, 22–34.

Eash, S., Manley, K., Gasparovic, M., Querbes, W., and Atwood, W.J. (2006). The human polyomaviruses. Cell. Mol. Life Sci. *63*, 865–876.

Ebert, M.S., Neilson, J.R., and Sharp, P.A. (2007). MicroRNA sponges: competitive inhibitors of small RNAs in mammalian cells. Nat. Methods *4*, 721–726.

Grey, F., Meyers, H., White, E.A., Spector, D.H., and Nelson, J. (2007). A human cytomegalovirus-encoded microRNA regulates expression of multiple viral genes involved in replication. PLoS Pathog. *3*, e163. 10.1371/journal.ppat.0030163.

Guo, H., Ingolia, N.T., Weissman, J.S., and Bartel, D.P. (2010). Mammalian microRNAs predominantly act to decrease target mRNA levels. Nature *466*, 835–840.

Jiang, M., Abend, J.R., Johnson, S.F., and Imperiale, M.J. (2009). The role of polyomaviruses in human disease. Virology *384*, 266–273.

Johnson, E.M. (2010). Structural evaluation of new human polyomaviruses provides clues to pathobiology. Trends Microbiol. *18*, 215–223.

Liu, C.K., and Atwood, W.J. (2001). Propagation and assay of the JC virus. Methods Mol. Biol. *165*, 9–17.

Mandelboim, O., Reyburn, H.T., Vales-Gomez, M., Pazmany, L., Colonna, M., Borsellino, G., and Strominger, J.L. (1996). Protection from lysis by natural killer cells of group 1 and 2 specificity is mediated by residue 80 in human histocompatibility leukocyte antigen C alleles and also occurs with empty major histocompatibility complex molecules. J. Exp. Med. *184*, 913–922.

Moens, U., and Johannessen, M. (2008). Human polyomaviruses and cancer: expanding repertoire. J. Dtsch. Dermatol. Ges. *6*, 704–708.

Nachmani, D., Stern-Ginossar, N., Sarid, R., and Mandelboim, O. (2009). Diverse herpesvirus microRNAs target the stress-induced immune ligand MICB to escape recognition by natural killer cells. Cell Host Microbe *5*, 376–385.

Nachmani, D., Lankry, D., Wolf, D.G., and Mandelboim, O. (2010). The human cytomegalovirus microRNA miR-UL112 acts synergistically with a cellular microRNA to escape immune elimination. Nat. Immunol. *11*, 806–813.

Nickeleit, V., Hirsch, H.H., Binet, I.F., Gudat, F., Prince, O., Dalquen, P., Thiel, G., and Mihatsch, M.J. (1999). Polyomavirus infection of renal allograft recipients: from latent infection to manifest disease. J. Am. Soc. Nephrol. *10*, 1080–1089.

O'Connell, R.M., Rao, D.S., Chaudhuri, A.A., and Baltimore, D. (2010). Physiological and pathological roles for microRNAs in the immune system. Nat. Rev. *10*, 111–122.

Raulet, D.H. (2003). Roles of the NKG2D immunoreceptor and its ligands. Nat. Rev. *3*, 781–790.

Seo, G.J., Fink, L.H., O'Hara, B., Atwood, W.J., and Sullivan, C.S. (2008). Evolutionarily conserved function of a viral microRNA. J. Virol. *82*, 9823–9828.

Skalsky, R.L., and Cullen, B.R. (2010). Viruses, microRNAs, and host interactions. Annu. Rev. Microbiol. *64*, 123–141.

Speck, S.H., and Ganem, D. (2010). Viral latency and its regulation: lessons from the gamma-herpesviruses. Cell Host Microbe *8*, 100–115.

Stern-Ginossar, N., Elefant, N., Zimmermann, A., Wolf, D.G., Saleh, N., Biton, M., Horwitz, E., Prokocimer, Z., Prichard, M., Hahn, G., et al. (2007). Host immune system gene targeting by a viral miRNA. Science *317*, 376–381.

Stern-Ginossar, N., Gur, C., Biton, M., Horwitz, E., Elboim, M., Stanietsky, N., Mandelboim, M., and Mandelboim, O. (2008). Human microRNAs regulate stress-induced immune responses mediated by the receptor NKG2D. Nat. Immunol. *9*, 1065–1073.

Stern-Ginossar, N., Saleh, N., Goldberg, M.D., Prichard, M., Wolf, D.G., and Mandelboim, O. (2009). Analysis of human cytomegalovirus-encoded microRNA activity during infection. J. Virol. *83*, 10684–10693.

Sullivan, C.S., Grundhoff, A.T., Tevethia, S., Pipas, J.M., and Ganem, D. (2005). SV40-encoded microRNAs regulate viral gene expression and reduce susceptibility to cytotoxic T cells. Nature *435*, 682–686.

Umbach, J.L., and Cullen, B.R. (2009). The role of RNAi and microRNAs in animal virus replication and antiviral immunity. Genes Dev. *23*, 1151–1164.

van de Wetering, M., Oving, I., Muncan, V., Pon Fong, M.T., Brantjes, H., van Leenen, D., Holstege, F.C., Brummelkamp, T.R., Agami, R., and Clevers, H. (2003). Specific inhibition of gene expression using a stably integrated, inducible small-interfering-RNA vector. EMBO Rep. *4*, 609–615.

Xu, K., Ma, H., McCown, T.J., Verma, I.M., and Kafri, T. (2001). Generation of a stable cell line producing high-titer self-inactivating lentiviral vectors. Mol. Ther. *3*, 97–104.